# NASA

# MEMORANDUM

## PERFORMANCE CHARACTERISTICS OF FLUSH AND SHIELDED AUXILIARY EXITS AT MACH NUMBERS OF 1.5 TO 2.0

By Kaleel L. Abdalla

Lewis Research Center
Cleveland, Ohio

NATIONAL AERONAUTICS AND SPACE ADMINISTRATION

WASHINGTON

June 1959

Declassified July 11, 1961

NATIONAL AERONAUTICS AND SPACE ADMINISTRATION

MEMORANDUM 5-18-59E

# PERFORMANCE CHARACTERISTICS OF FLUSH AND SHIELDED AUXILIARY EXITS AT MACH NUMBERS OF 1.5 TO 2.0

By Kaleel L. Abdalla

## SUMMARY

The performance characteristics of several flush and shielded auxiliary exits were investigated at Mach numbers of 1.5 to 2.0, and jet pressure ratios from jet off to 10.

The results indicate that the shielded configurations produced better over-all performance than the corresponding flush exits over the Mach-number and pressure-ratio ranges investigated. Furthermore, the full-length shielded exit was highest in performance of all the configurations. The flat-exit nozzle block provided considerably improved performance compared with the curved-exit nozzle block.

## INTRODUCTION

For high Mach number turbojet aircraft, studies of the inlet-engine matching problem have shown that optimum powerplant thrust minus drag at off-design speeds can be obtained if the inlet is permitted to capture more air than the engine can handle (ref. 1). In this "bypass" matching method the excess air is returned to the free stream and the auxiliary exit that performs this function must have high performance for good over-all powerplant performance.

General performance characteristics and design criteria for auxiliary exits are reported in references 2 and 3. In the present investigation the over-all performance of several auxiliary-exit designs was obtained by mounting the exits on a simulated fuselage and by designing the nozzles to handle typically required bypass flows.

Several flush exits and shielded oblique exits were investigated in the NASA Lewis 8- by 6-foot supersonic wind tunnel to determine the thrust and drag performance with the simulated fuselage. Data were taken at Mach numbers of 2.0, 1.8, and 1.5 at zero angle of attack. The ratio of jet total pressure to free-stream static pressure was varied from jet off to 10.

## SYMBOLS

| | |
|---|---|
| $A$ | cross-sectional area |
| $A_{ti}$ | ideal exit area of convergent nozzle |
| $D$ | drag |
| $D_n$ | exit nozzle-block drag, based on projected area |
| $D_s$ | shield drag, based on projected area |
| $F$ | thrust |
| $F_{ic}$ | ideal jet thrust of convergent nozzle |
| $F_j$ | jet thrust |
| $g$ | gravitational constant, 32.17 $ft/sec^2$ |
| $M$ | Mach number |
| $P$ | total pressure |
| $P_j/p_0$ | jet pressure ratio, jet total to free-stream static pressure ratio |
| $p$ | static pressure |
| $p_{ei}$ | ideal exit static pressure of convergent nozzle |
| $V_{ti}$ | ideal exit velocity of convergent nozzle |
| $w$ | weight flow rate, lb/sec |
| $\theta$ | exit flow angle, deg |

Subscripts:

| | |
|---|---|
| b | base |
| i | ideal |
| j | jet exit conditions |
| t | throat conditions |
| w | conditions on exit nozzle-block wall |
| 0 | free-stream conditions |

## APPARATUS

A schematic diagram of the auxiliary-exit-model installation in the wind tunnel is shown in figure 1, and model details are shown in figure 2. The model consisted of a 10° half-angle conical nose section and an 8-inch outside diameter cylindrical body. The auxiliary-exit shields and flush exits were mounted in the aft-section of the model as shown in figure 2. The model total length was 71.0 inches. Predried air was supplied to the model internally through the support struts.

Figure 2 shows the grounded and ungrounded sections of the model as well as the strain-gage balance and pressurized bellows. It can be seen that the balance measures forces on the entire external skin and the base as well as the internal nozzle forces. A description of the balance system is given in reference 4.

### Configurations

The auxiliary exit configurations consisted of five shielded and flush exits combined with two exit nozzle-block designs. The nozzles were basically two dimensional and were faired into the axisymmetric fuselage. The two nozzle-block designs are shown schematically in figure 3. The auxiliary-exit configurations are drawn to scale in figure 4, and nozzle areas are also shown in the table in this figure. The flush-type auxiliary exit is designed to simulate a fully open (model 1) and a partially open (models 2 and 3) sliding-door bypass mechanism. The fully shielded exits (models 6 and 7) simulate a hinged bypass with full side fairings opened 15° into the airstream. Two combinations of these types of exits are also shown. One arrangement is a partially opened sliding door with side fairings swung 15° to the free stream (models 4 and 5). The second is a full-length curved-lip shield with partial side fairings hinged 15° to the stream (model 8). Photographs of typical configurations are shown in figure 5.

### Instrumentation and Data Reduction

The skin friction and pressure drag of the basic model $D_0$ was determined with the exit sealed. The base drag was determined from eight static orifices and from the base area $A_b$. For all configurations at each pressure ratio, thrust minus drag was obtained from

$$F_j - D = F_{balance} - D_0 - (p_b - p_0)A_b$$

For the shielded configurations, shield drag was computed from nine area-weighted static orifices, and thrust was obtained by adding this drag to

the thrust minus drag. For all configurations the nozzle blocks were instrumentated with 15 static orifices along the centerline (see fig. 3).

Net jet weight flow was determined from the difference between the flow through the sharp-edged orifice plates in the air-supply line and and the calibrated-model leakage flow. Total temperature was obtained from thermocouples located in the pressure chamber inside the model, assuming constant temperature to the exit station. Internal-flow total pressure was averaged from a nine-tube total-pressure rake located at station 46.75 (see fig. 3).

Ideal convergent nozzle thrust was found from

$$F_{ic} = \frac{W}{g} V_{ti} + (p_{ei} - p_0)A_{ti}$$

where $V_{ti}$, $p_{ei}$, and $A_{ti}$ were computed from the measured weight flow, the measured temperature, and the measured jet total pressure assuming isentropic flow and $M_t = 1.0$. (Flow coefficients were 1.0 within experimental accuracy of data.)

Convergent thrust was used as a reference because the nozzles tested were basically convergent. For convenience the conversion factor between ideal convergent thrust and ideal thrust is plotted in figure 6.

## GENERAL CONSIDERATIONS

The flush and the shielded exits represent two basically different approaches to the auxiliary-exit problem. With the flush exits (see fig. 7(a)) pressures greater than ambient on the nozzle block just downstream of the throat represent drag. At jet pressure ratios above approximately 2, therefore, this drag will penalize the performance of the flush configurations. The drag is increased further by the external stream because of the higher local pressure behind the stream shock (fig. 7(a)). The higher local pressures prevent part of the expansion which would have occurred without stream effects, and result in higher nozzle-block pressures as indicated in the typical pressure distributions of figure 7(a). Since the area between any curve and a horizontal line at the particular value of $p_0/P_j$ is proportional to nozzle-block drag, it is clear that with an external stream the drag is higher and therefore thrust minus drag is lower. For the case illustrated the difference is proportional to the sum of areas A and B (fig. 7(a)).

With the fully shielded exits, jet-stream interaction has little or no effect on nozzle-block pressures (see fig. 7(b)). Also, side fairings on the full shields prevent escape of the exit flow around the sides (see fig. 5(a)). There is, however, drag on the shield, which must be compared with the nozzle-block drag of the flush exits. For both flush and shielded exits, of course, there are added losses resulting from the nonaxial exit.

## RESULTS AND DISCUSSION

### Flush Auxiliary Exits

The thrust-minus-drag characteristics for the three flush auxiliary exits are presented in figure 8. These flush exits exhibit relatively poor performance over the entire operating range investigated.

The poor performance must result from the nozzle-block drag, as well as from the nonaxial exit, as mentioned in the previous section. For the flush exits the nozzle-block drags, because of nozzle geometry, are higher than would be estimated by centerline pressure distributions. Since the auxiliary exits are basically two-dimensional, matching the exits to the axisymmetric fuselage resulted in considerably different nozzle-block cross sections near the sides compared with the centerline cross sections shown in figure 4 (see fig. 5(c)). As a result, jet flow away from the centerline, downstream of the throat, will not expand to ambient static pressures along the nozzle-block. On a unit-area basis, therefore, these higher static pressures away from the centerline produce higher nozzle-block drags than would be obtained from centerline pressure distributions.

In order to illustrate the relative magnitude of this effect on performance the centerline pressure distributions for model 1, shown in figure 9, were used to compute drag. Then, assuming a theoretical nozzle thrust coefficient of 0.98 and an effective flow angle at the throat of $19^{\circ}$, the thrust coefficient was 0.927 ($0.98 \times \cos 19^{\circ}$). The resulting estimated thrust minus drag is shown in figure 8 as the dashed line. It is clear that the off-centerline pressures must produce greater drag than the centerline pressures.

### Shielded Auxiliary Exits

The thrust and drag characteristics for the five shielded auxiliary exits are presented in figure 10. The thrust-minus-drag performance of the shielded configurations was considerably better than that of the corresponding flush exits. (Compare figs. 10 and 8.) Furthermore, the best thrust and thrust-minus-drag characteristics were obtained with full-length shielding because the exit flow expanded along the

nozzle-block wall with little or no jet-stream interaction, as exemplified by the exit nozzle-block pressure distributions of figure 11 (solid curve). The partially shielded configurations, of course, were susceptible to some jet-stream interaction, although the severity of this effect was less for these configurations than for the flush exits because of the oblique shields and side fairings.

For the curved-lip shielded exit only part of the shield had side fairings (see fig. 5(b)), and the nozzle-block pressure distribution (dashed curve of fig. 11) shows the more rapid expansion of the jet as as well as some stream interaction at low pressure ratios. The over-all performance of this configuration at the higher pressure ratios was penalized. Good thrust-minus-drag characteristics, however, were maintained at low pressure ratios. Thus, the improved over-all thrust-minus-drag performance of the shielded exits results from the fact that the shield drags were lower than the nozzle-block drags of the flush exits.

### Type of Exit Nozzle Block

The effect of the type of exit nozzle-block design can be seen by the comparison of flush and shielded configurations investigated with both the flat-exit nozzle block and the curved-exit nozzle block. (Compare the thrust-minus-drag performance of models 2 and 3 (fig. 8), models 4 and 5, and models 6 and 7 (fig. 10).) In general, the over-all performance of a configuration with the flat nozzle block is appreciably better than that of the similar configuration with the curved nozzle block.

## SUMMARY OF RESULTS

The investigation of the performance characteristics of several flush and shielded exhaust nozzles in a supersonic stream indicates:

1. The shielded oblique exhaust nozzles produce a higher thrust-minus-drag performance than the corresponding flush exits.

2. Although for the curved-lip shielded configuration the low pressure ratio thrust-minus-drag performance was improved, the best over-all performance was obtained with full-length shielding.

3. The performance of a configuration with the flat-exit nozzle block is appreciably better than that of a similar configuration with the curved-exit nozzle block.

Lewis Research Center
National Aeronautics and Space Administration
Cleveland, Ohio, February 26, 1958

## REFERENCES

1. Hearth, Donald P.: Use of Main-Inlet Bypass to Supply Ejector Exhaust Nozzle at Supersonic Speeds. NACA RM E56K08, 1957.

2. McLafferty, G. H., et al.: Investigation of Turbojet Inlet Design Parameters. R-0790-13, United Aircraft Corp., Dec. 1955.

3. Anderson, D. C.: Efficiency of Flush and Protruding Oblique Exhaust Nozzles With and Without External Flow. United Aircraft Corp. R-0955-22, 1957. (Unclassified).

4. Valerino, Alfred S., Zappa, Robert F., and Abdalla, Kaleel L.: Effects of External Stream on the Performance of Isentropic Plug-Type Nozzles at Mach Numbers of 2.0, 1.8, and 1.5. NASA MEMO 2-17-59E, 1959.

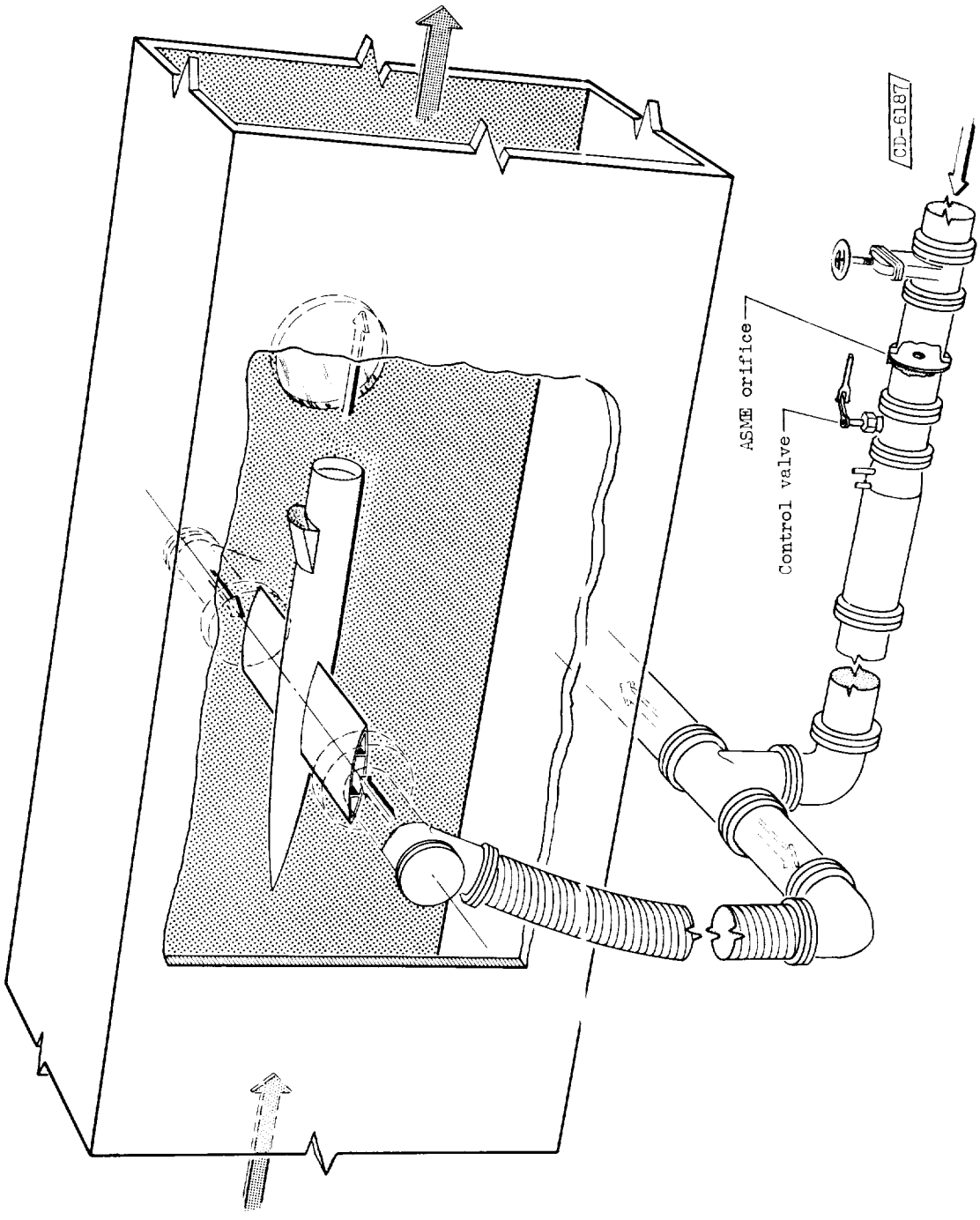


Figure 1. - Schematic diagram of auxiliary-exit-model installation in tunnel.

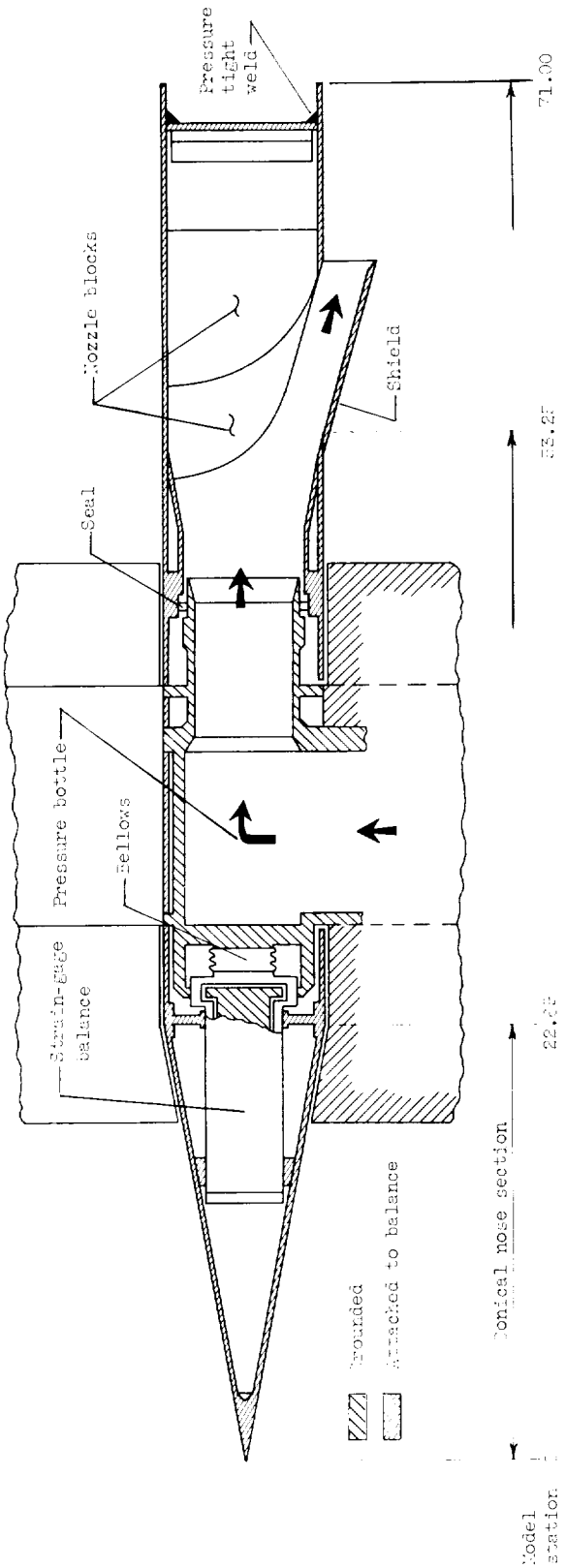


Figure 2. - Schematic diagram of auxiliary-exit model.

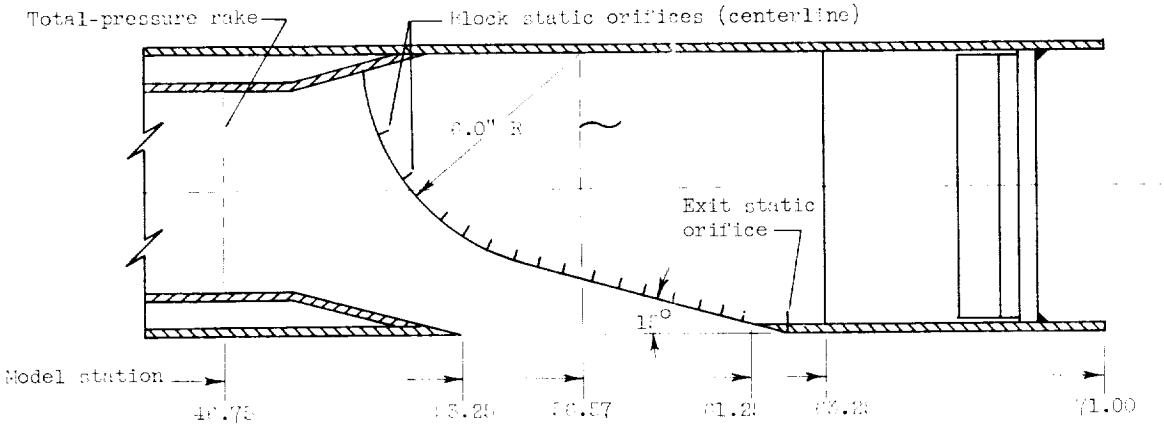


(a) Flat-exit nozzle block.

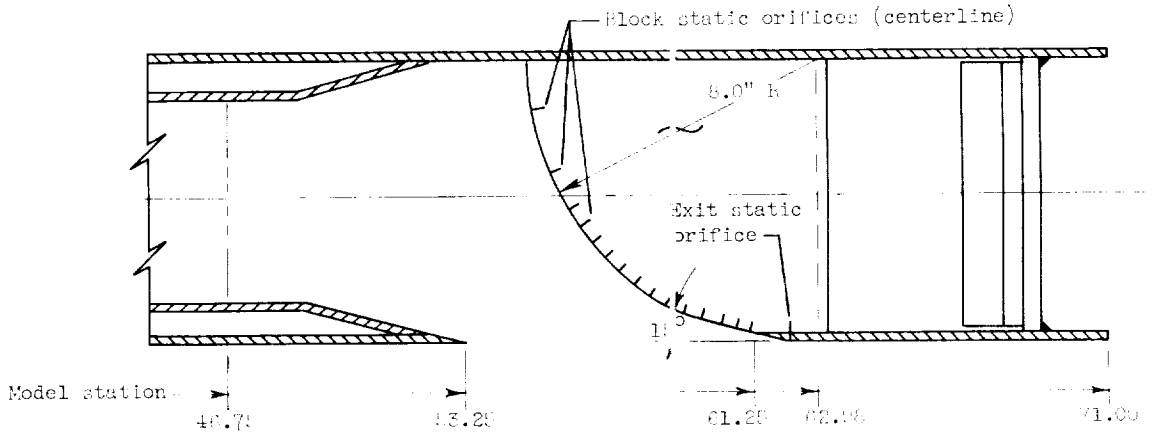


(b) Curved-exit nozzle block.

Figure 3. - Schematic diagram of exit nozzle block showing location of static orificies. Centerline cross section.

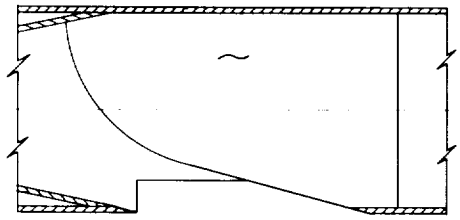

Exit model 1. Basic, no shield, flat nozzle block

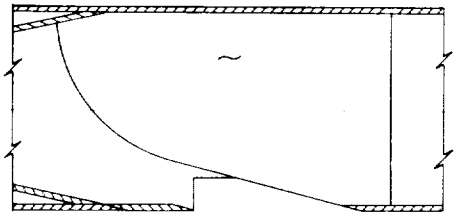

Exit model 2. Flush shield, flat nozzle block

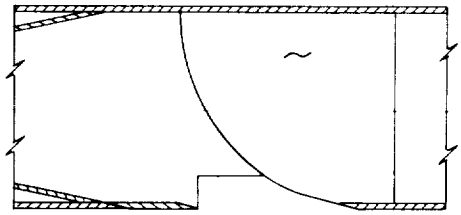

Exit model 3. Flush shield, curved nozzle block

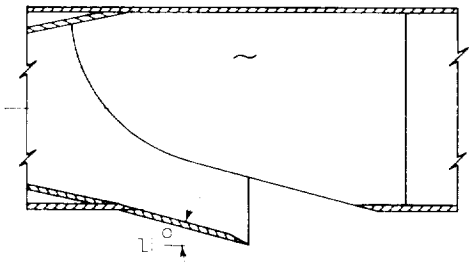

Exit model 4. Partially hinged shield, flat nozzle block

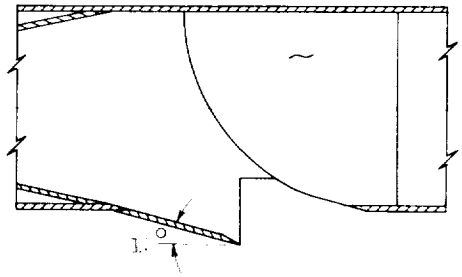

Exit model 5. Partially hinged shield, curved nozzle block

(a) Schematic diagrams of configurations. Centerline cross sections.

Figure 4. - Configurations and nozzle areas.

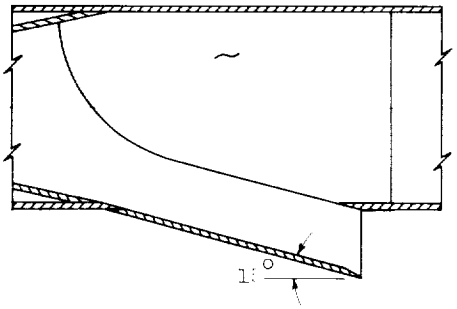


Exit model 6. Fully hinged shield, flat nozzle block

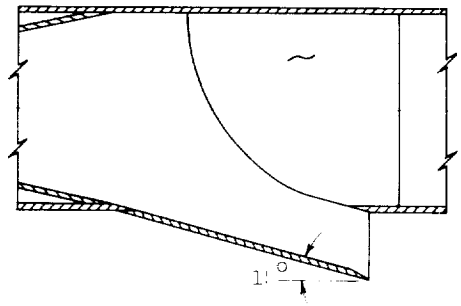


Exit model 7. Fully hinged shield, curved nozzle block

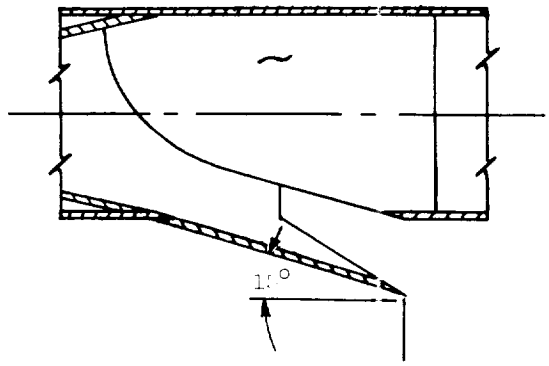


Exit model 8. Hinged curved-lip shield, flat nozzle block

01-1368

Table I

| Exit model | Model station, in. | Nozzle throat area, sq. ft. | Shield projected area sq. ft. |
|---|---|---|---|
| 1 | 53.28 | 0.0825 | 0 |
| 2 | 56.00 | .0873 | 0 |
| 3 | 56.00 | .0874 | 0 |
| 4 | 57.10 | .0772 | .0804 |
| 5 | 57.10 | .0873 | .0504 |
| 6 | 61.28 | .0778 | .0947 |
| 7 | 61.28 | .0892 | .0847 |
| 8 | 61.28 | .0780 | .0787 |

(b) Table of nozzle areas.

Figure 4. - Concluded. Configurations and nozzle areas.

(a) Model 6. Fully shielded exit with flat nozzle block.

(b) Model 8. Curved-lip-shielded exit with flat nozzle block.

Figure 5. - Typical auxiliary-exit configurations.

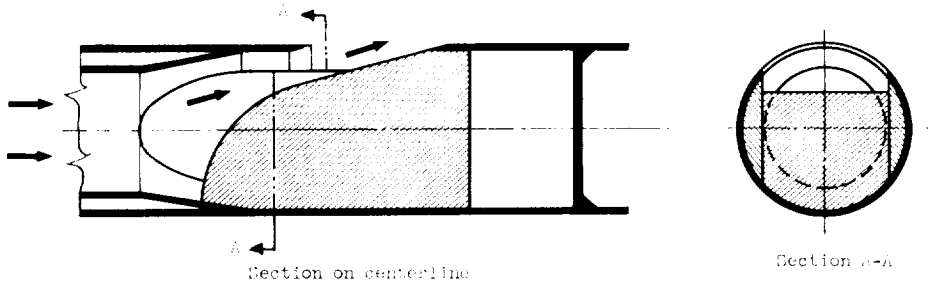


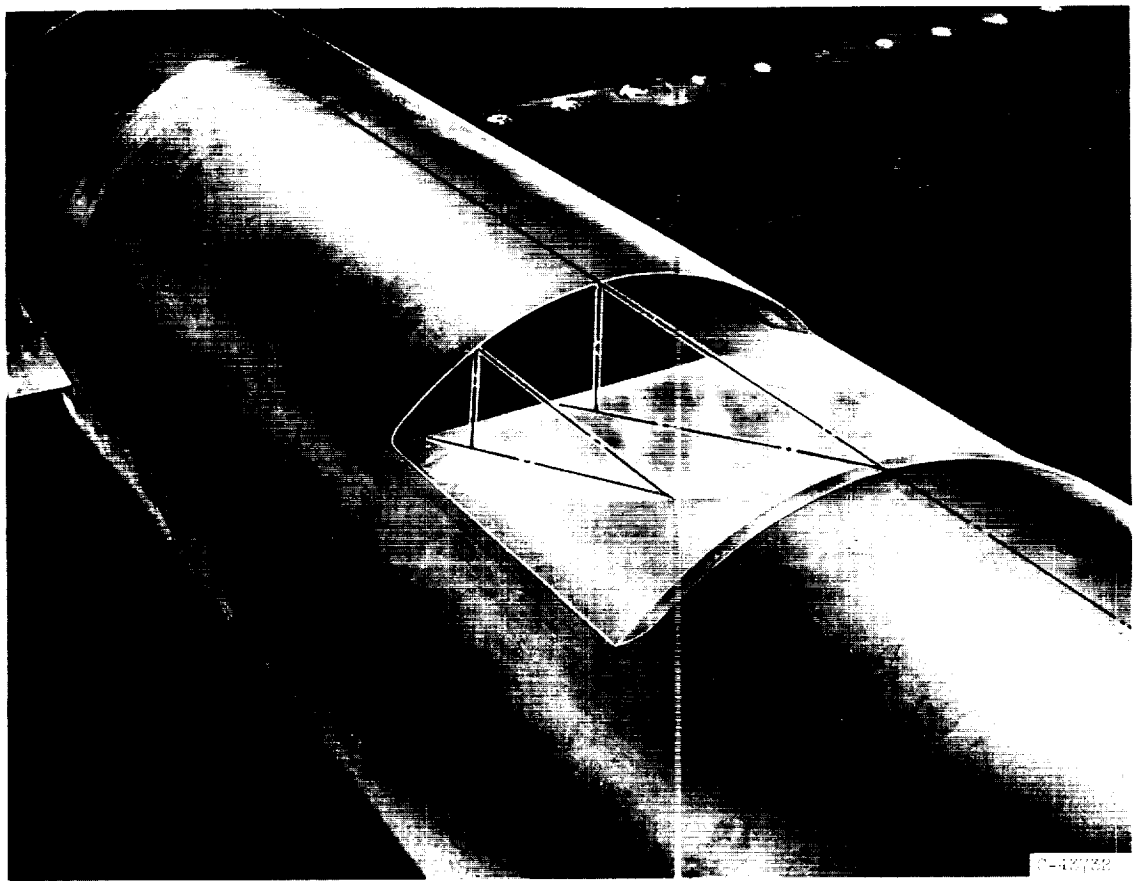

(c) Model 2. Two-dimensional nozzle sized to the axisymmetric fuselage. (Retouched photograph.)

Figure 5. - Concluded. Typical auxiliary-exit configurations.

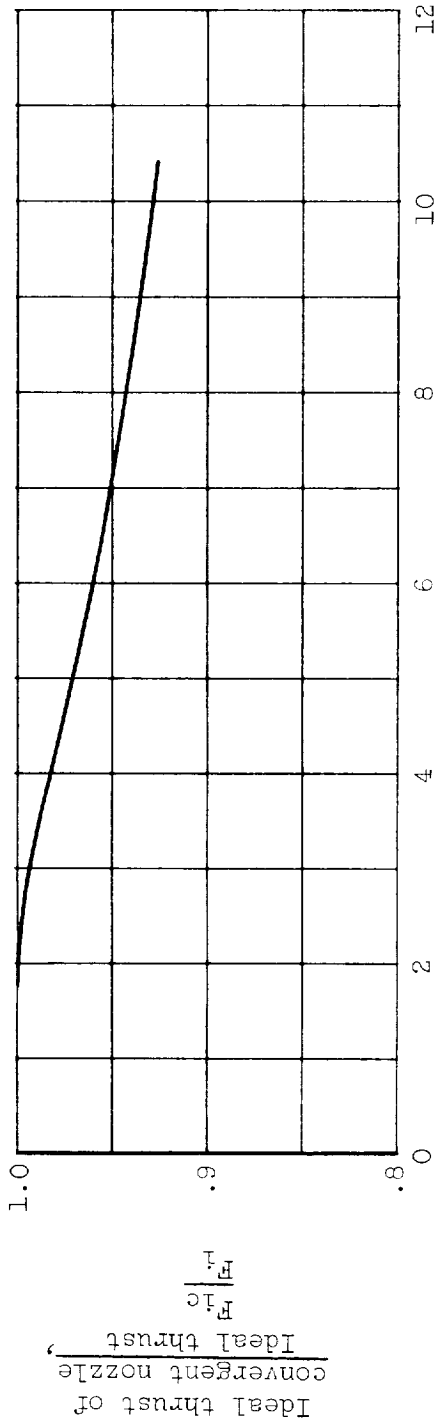


Figure 6. - Relation between convergent ideal thrust and ideal thrust.

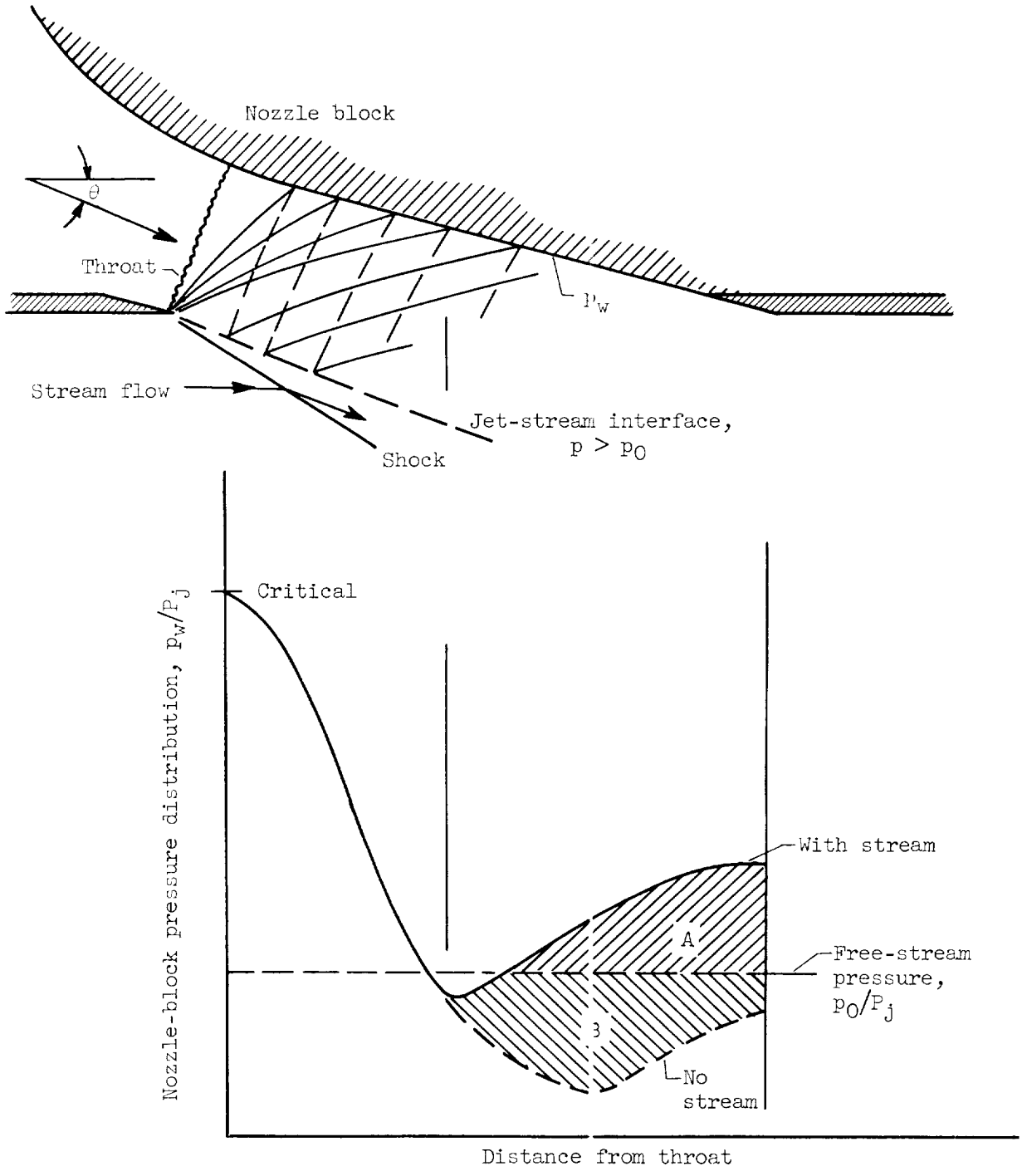


(a) Flush-type exit.

Figure 7. - Nozzle centerline pressure distribution and stream effects on exits.

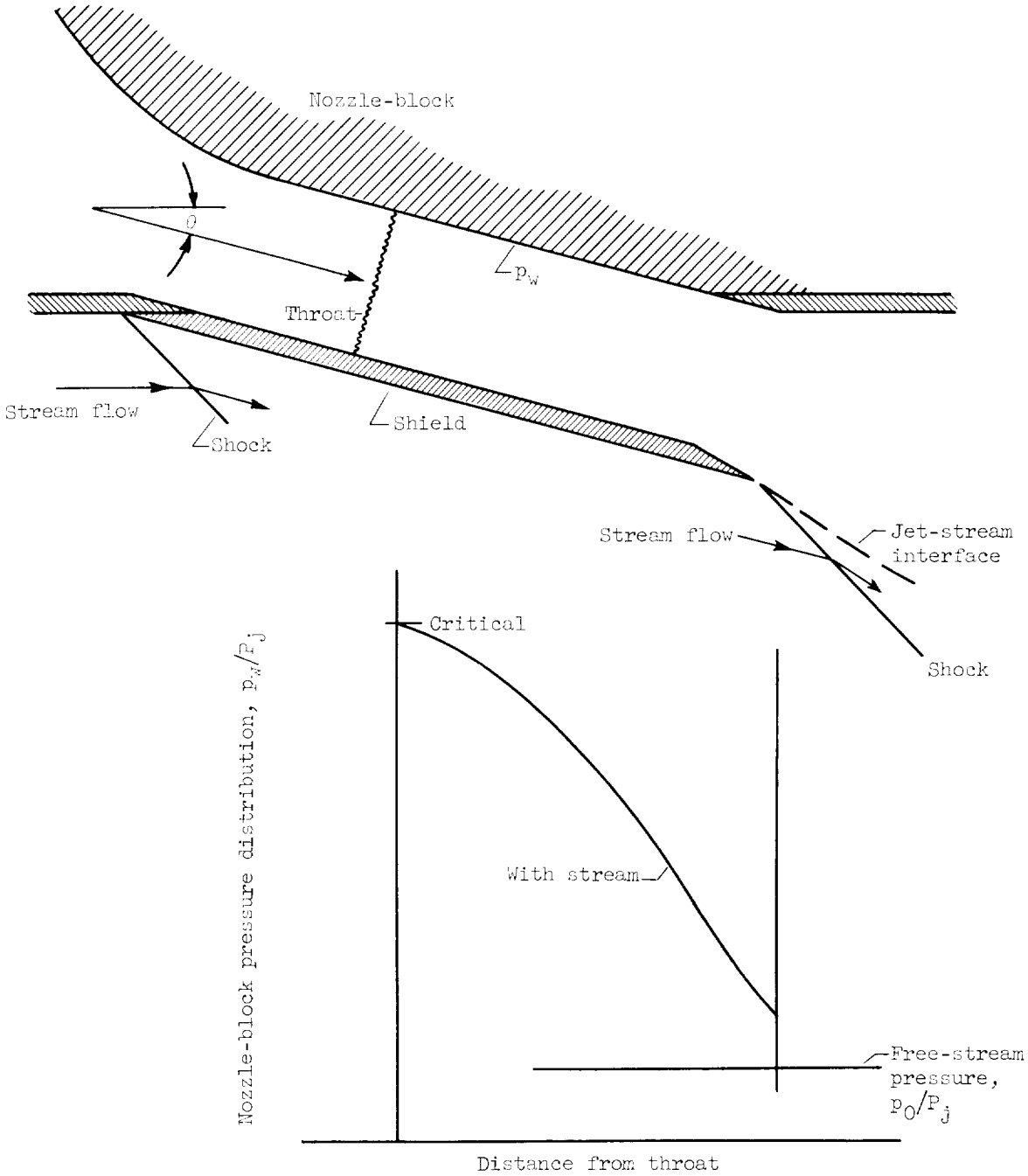


(b) Shielded exits.

Figure 7. - Concluded. Nozzle centerline pressure distribution and stream effects on exits.

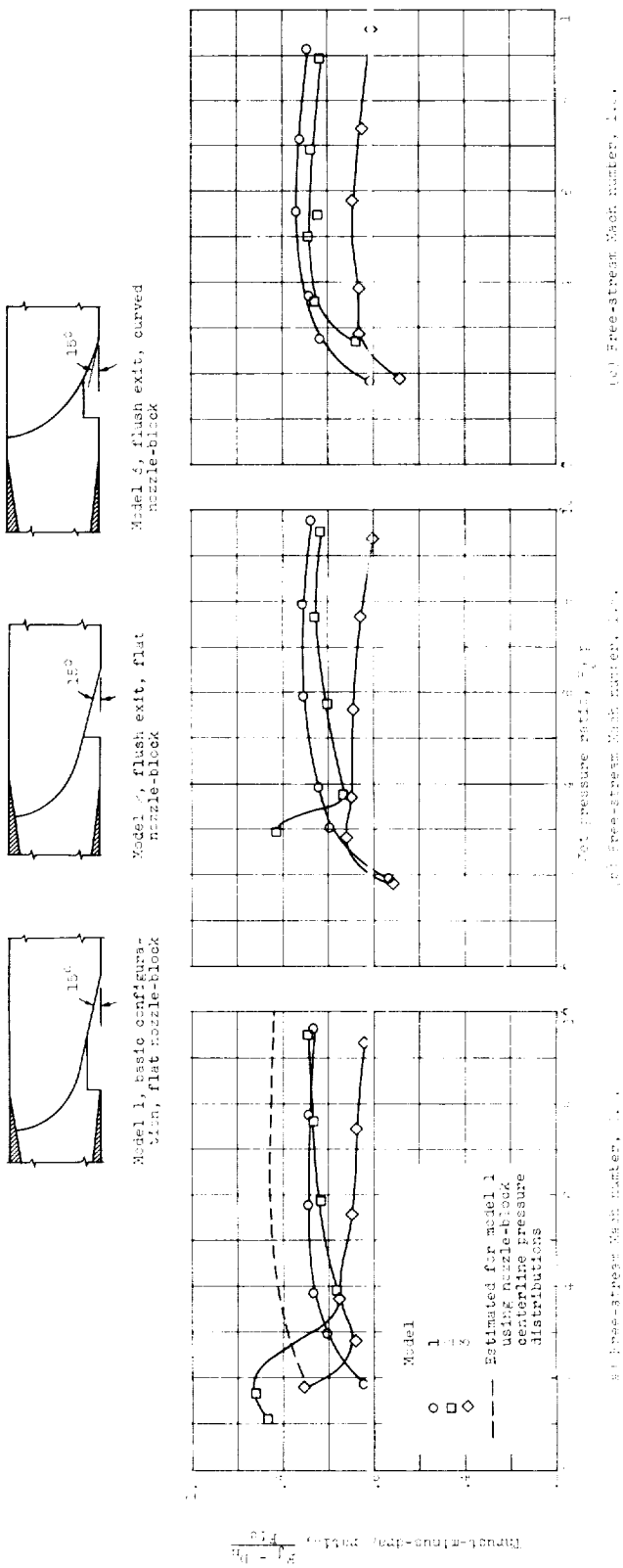


Figure 8. - Thrust and drag characteristics of flush auxiliary exits.

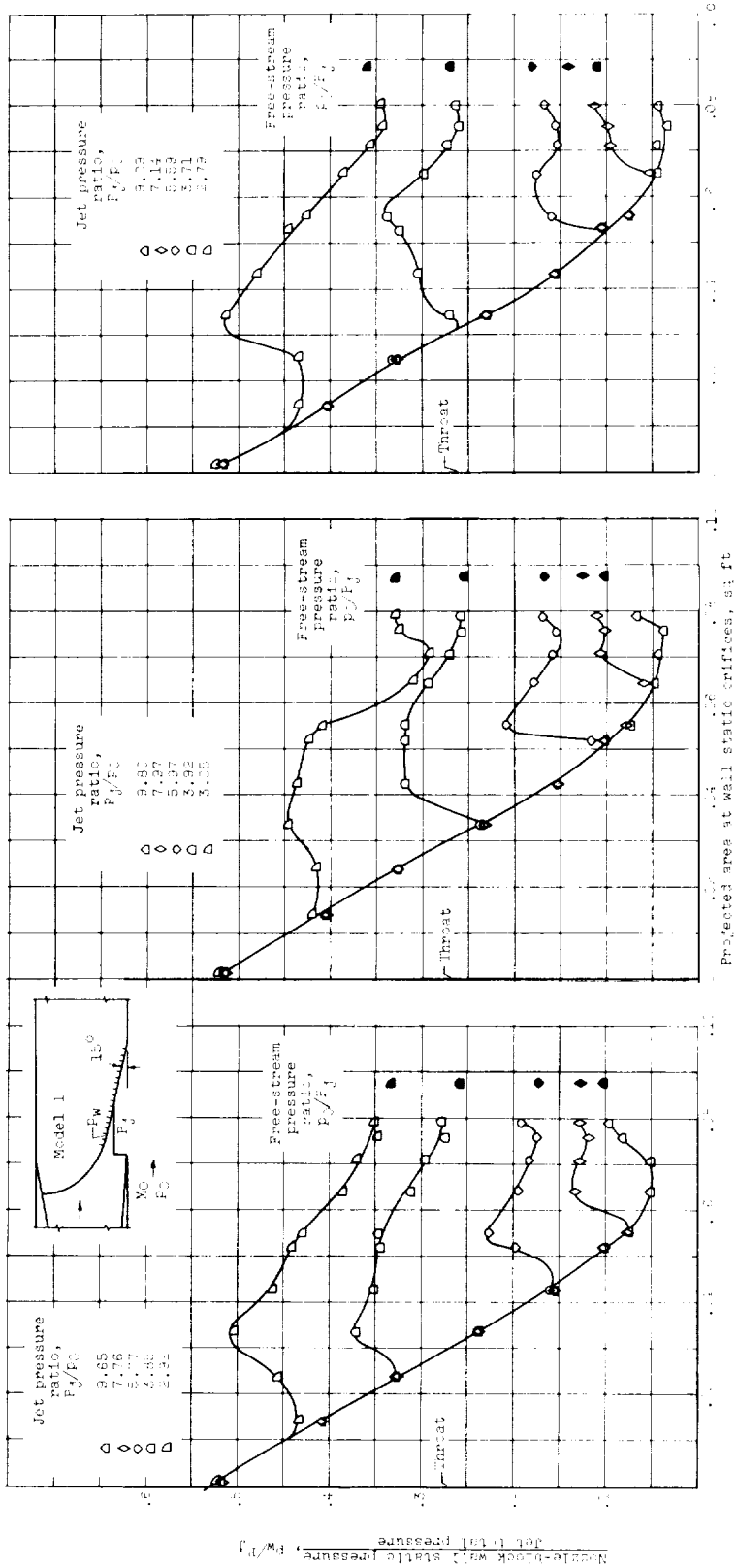


Figure 9. - Typical exit nozzle-block centerline pressure distributions for flush exits (model 1).

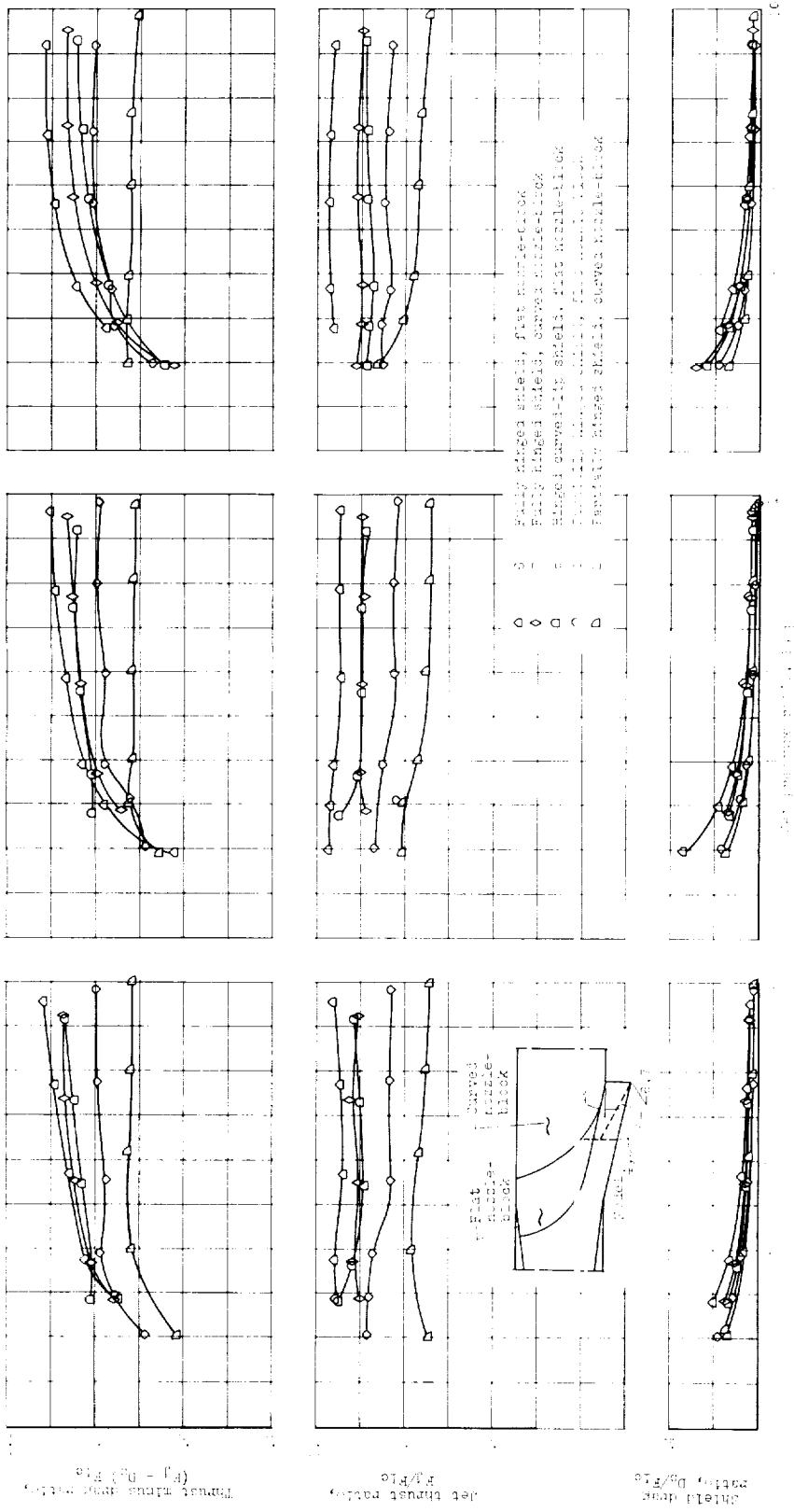

Figure 10. - Thrust and drag characteristics of shielded auxiliary exits.

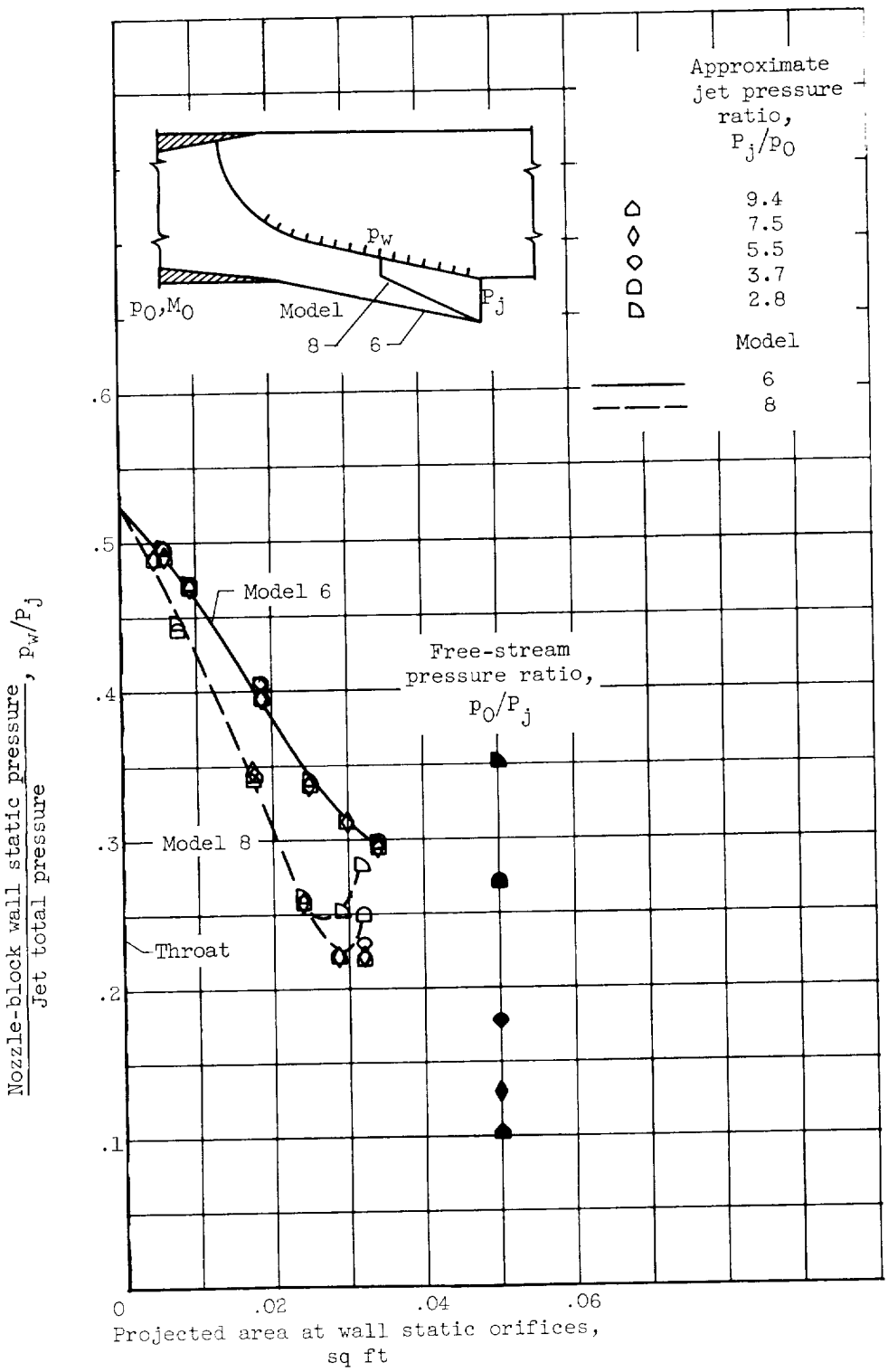


Figure 11. - Exit nozzle-block centerline pressure distributions. Free-stream Mach number, 2.0; shielded exits.